

# Feasibility of an ultra-low power digital signal processor platform as a basis for a fully implantable brain-computer interface system

Po T. Wang<sup>1</sup>, Keulanna Gandasetiawan<sup>2</sup>, Colin M. McCrimmon<sup>1</sup>, Alireza Karimi-Bidhendi<sup>3</sup>, Charles Y. Liu<sup>4</sup>, Payam Heydari<sup>3</sup>, Zoran Nenadic<sup>1,3</sup>, An H. Do<sup>5</sup>

**Abstract**—A fully implantable brain-computer interface (BCI) can be a practical tool to restore independence to those affected by spinal cord injury. We envision that such a BCI system will invasively acquire brain signals (e.g. electrocorticogram) and translate them into control commands for external prostheses. The feasibility of such a system was tested by implementing its benchtop analogue, centered around a commercial, ultra-low power (ULP) digital signal processor (DSP, TMS320C5517, Texas Instruments). A suite of signal processing and BCI algorithms, including (de)multiplexing, Fast Fourier Transform, power spectral density, principal component analysis, linear discriminant analysis, Bayes rule, and finite state machine was implemented and tested in the DSP. The system’s signal acquisition fidelity was tested and characterized by acquiring harmonic signals from a function generator. In addition, the BCI decoding performance was tested, first with signals from a function generator, and subsequently using human electroencephalogram (EEG) during eyes opening and closing task. On average, the system spent 322 ms to process and analyze 2 s of data. Crosstalk ( $<-65$  dB) and harmonic distortion ( $\sim 1\%$ ) were minimal. Timing jitter averaged 49  $\mu$ s per 1000 ms. The online BCI decoding accuracies were 100% for both function generator and EEG data. These results show that a complex BCI algorithm can be executed on an ULP DSP without compromising performance. This suggests that the proposed hardware platform may be used as a basis for future, fully implantable BCI systems.

## I. INTRODUCTION

Every year, between 250,000 and 500,000 people in the world suffer a spinal cord injury (SCI), which can lead to permanent disability [1]. Paralysis due to SCI decreases quality of life for the affected individuals and their family members and can lead to medical complications such as cardiovascular problems and pressure ulcers. In the US alone, the primary and secondary health care costs associated with SCI are estimated to be  $\sim$ \$50 billion per year [2]. Thus, practical solutions for restoring motor functions after SCI are desperately needed. Brain-computer interfaces (BCI) can be used to bypass the damaged spinal cord and facilitate direct brain-control of prosthetic devices such as exoskeletons

or functional electrical stimulation systems. Recent studies have shown that using invasively acquired electrocorticogram (ECoG) signals is promising for BCI application [3], [4]. However, such ECoG-based BCIs utilize large, power-hungry electronics and external computers, which limit their use to lab settings only. Some researchers proposed to address this problem by developing intracranial implants capable of acquiring brain signals and wirelessly transmitting them to an external computer for processing [5], [6]. However, this approach does not fundamentally circumvent the reliance on an external computer. Furthermore, such bulky systems are unlikely to gain a widespread adoption by the target patient population. Therefore, a practical low power BCI that is highly portable, always available, and aesthetically pleasing must be developed.

We hypothesize that all of these criteria can be met with a fully implantable ECoG-based BCI (Fig. 1A). This system is envisioned to include a skull unit, which is used to amplify and serialize up to 64-channel electrocorticogram (ECoG) signals into a single channel. These signals are routed to a chest wall unit (CWU), which digitizes, de-multiplexes, and processes the signals to decode the underlying intentions (Fig. 1B). The digitizer is designed to capture up to the high- $\gamma$  band (80–160 Hz), which is known to modulate with movements [3], [4]. The CWU also includes a wireless transceiver to facilitate communication with external prosthetic devices and diagnostic units. The entire system is expected to be powered by a battery with wireless recharging capability. The fully implantable nature of this system will make it highly portable and always available. Furthermore, the absence of any transcutaneous electronic components greatly mitigates the infection risk and makes the system aesthetically acceptable to potential recipients. In this study, we developed a benchtop analogue of this proposed fully implantable BCI system and validated its functions with artificial signals as well as with human electroencephalogram (EEG) signals.

## II. METHODS

To mimic the function of a fully implantable BCI system, a custom amplifier array and multiplexer (mux) were used as an analogue to the skull unit, and an ultra-low power (ULP) digital signal processor (DSP) development board was used to simulate the CWU. The DSP was programmed with a custom BCI algorithm, and this system’s functions were tested using artificial and human EEG signals. The system

This work was funded by the National Science Foundation, Award #1446908

<sup>1</sup>Dept. of Biomedical Engineering, University of California, Irvine, CA 92697 USA. {ptwang, cmccrimm, znenadic}@uci.edu

<sup>2</sup>Dept. of Computer Science, University of California, Irvine, CA 92697 USA. keulanna@uci.edu

<sup>3</sup>Dept. of Electrical Engineering and Computer Science, University of California, Irvine, CA 92697 USA. {akarimib, payam}@uci.edu

<sup>4</sup>Dept. of Neurosurgery, University of Southern California, Los Angeles, CA 90033 USA. chasliu@cheme.caltech.edu

<sup>5</sup>Dept. of Neurology, University of California, Irvine, CA 92697 USA. and@uci.edu

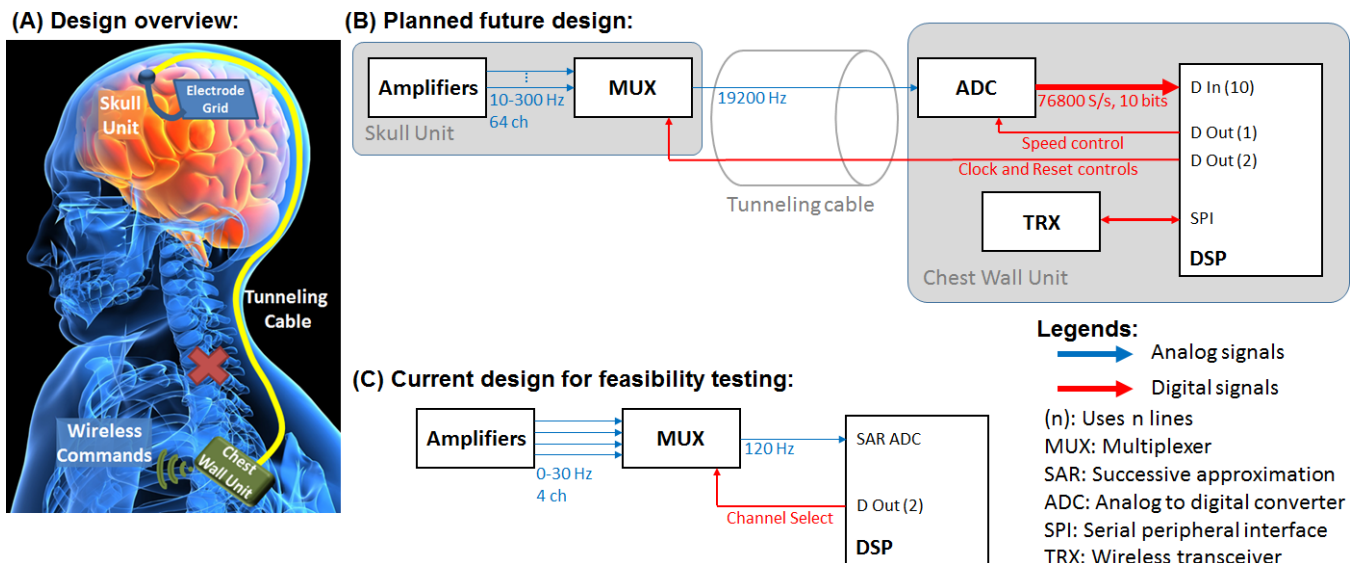


Fig. 1. (A) Design overview and (B) schematic of the future fully implantable BCI system. (C) Design of the benchtop analogue tested in the present study. Frequency values indicate bandwidth.

performance was used to determine this platform can be used as a basis for a fully implantable BCI system.

### A. Design

A commercially available development board (EVM5517, Spectrum Digital Inc, Stafford, TX) for the TMS320C5517 (“C5517”, Texas Instruments, Dallas, TX) DSP was connected to a 4-channel mux (MAX4618, Maxim Integrated, San Jose, CA). The mux was then connected to either a function generator or a custom EEG amplifier for testing (described further below). This setup was implemented on prototyping boards.

Consistent with our previous EEG-based BCI systems [7], [8], the basic function of the proposed system is to be able to decode a user’s brain signals into one of two states. To this end, the BCI was designed to operate in two modes. First, a training mode involves collecting brain signals while cuing the user to perform idling or moving tasks. Then, in the online mode, the BCI predicts the state from brain signals acquired in real time. Common to both modes of operation are the following signal acquisition and processing procedures. Digitized 10-bit signals from the C5517’s analog-to-digital-converter (ADC) were stored in a pair of 16-bit unsigned integer arrays with additional meta-data embedded in the unused bits (Fig. 2). These arrays were stored in the DSP’s internal random access memory (RAM), allowing the BCI to run at high speed. They were also written into an SD card (serving as an analogue for an embedded MMC storage module in a future fully implantable BCI system), which facilitates the system’s ability to perform long-term ECoG recordings. Signals were subsequently demultiplexed and converted to power spectral densities (PSD) using Fast Fourier Transform (FFT). The PSD were then binned into the following EEG bands:  $\alpha$  (8–12 Hz), low- $\beta$  (12–20 Hz), high- $\beta$  (20–30 Hz), and low- $\gamma$  (30–40 Hz).

During training, 40-s of signals underlying the state A and 40-s underlying state B were collected to train the BCI decoder. Specifically, the binned PSD underlying the two states were used to derive dimensionality reduction transformation consisting of a combination of principal component analysis (PCA, set to retain 99.7% of variances) and linear discriminant analysis (LDA). This resulted in a dimensionality reduction from 16 D (4 bins  $\times$  4 channels) to 1 D. The class-specific means and variances of these 1 D features were then used to obtain the posterior probability of each class by utilizing the Bayes rule with unpooled Gaussian likelihoods and equal priors. Similar to out prior EEG-based BCIs [7], [8], the current BCI’s online mode was modeled as a binary state machine with the state transition parameters established through a calibration procedure. To this end, 20-s long signal samples underlying each state were acquired and processed in the frequency domain in the same manner as the training data above. Upon transforming these calibration samples into 1 D features, the Bayes rule was applied to obtain the posterior probability of state B given feature  $f$ ,  $P(B|f)$ . Note that  $P(A|f) = 1 - P(B|f)$ . For each state, the average of  $P(B|f)$  was calculated and used as the state machine transition threshold, i.e.  $T_A = \text{mean}\{P(B|f \in A)\}$  and  $T_B = \text{mean}\{P(B|f \in B)\}$ .

In the online mode, 2-s long data windows were processed in the same manner as the calibration data. The posterior probability,  $P(B|f)$ , was calculated using the Bayes rule and compared to the state transition thresholds in real time. If  $P(B|f) \leq T_A$ , the state machine either remains in state A or switches from state B to A. If  $P(B|f) \geq T_B$ , the state machine either remains in state B or switches from state A to B. If  $T_A < P(B|f) < T_B$ , the BCI defaults to the current state. Note that these state transition rules allow the state to be maintained without having to keep the posterior probability constantly above or below the respective

threshold. In this study, BCI outputs were streamed to the debug console on a desktop computer in order to monitor the BCI system’s performance. The details of these operations are illustrated in Fig. 3.

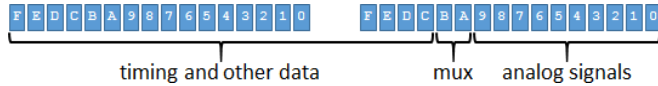


Fig. 2. Data storage structure for one sample. The first 10 bits store the signal. The next 2 bits store the mux state (which channel). The last 20 bits store the differential elapsed time of each sample in units of 1/50 ms and can also be used to store other meta-data.

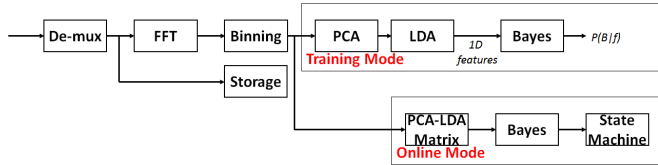


Fig. 3. Software design block diagram.

### B. Function Generator Test

The BCI system was first tested using artificial signals to ascertain its ability to reproduce and decode the acquired signals. To this end, a function generator was used to generate 100 mVpp sine wave signals with various frequencies at 400 mV offset. The signals were acquired through one of the mux input channel, while the remaining 3 channels were grounded. Signals were recorded at 4000 Hz and subsequently exported via the SD card for analysis. Time domain plots and power spectrum were used to assess signal acquisition fidelity, cross-talk specification, total harmonic distortion (THD) and the correct encoding of mux and timing meta-data.

Next, BCI operation was also tested by using a sine wave to simulate the brain signals underlying state A and a square wave of the same frequency to simulate brain signals underlying state B. These signals were generated during the training mode, and a BCI decoding model was generated as described above. During the online mode test, alternating 20-s long periods of sine and square waves were sent to the system while the BCI decoded the signals in real time. This was repeated for a total of 200 seconds. The number of correctly decoded samples as well as the total number of decoded samples were recorded to ascertain the system’s performance.

Both the signal fidelity and BCI tests were performed at 13, 113, and 223 Hz.

### C. Human EEG Test

A custom-made 4-channel bio-amplifier [9] was connected to the 4 channels on the mux. Note that signal fidelity was not examined here, as this has already been tested in [9].

The system’s ability to decode brain signals was tested with human EEG. An able-bodied male subject (20 yo) underwent EEG placement over electrodes Oz, O1, O2, and POz (referenced to AFz) according to the 10-20 international

TABLE I

THE SINE WAVE TEST WAS CONDUCTED AT 4000 HZ SAMPLE RATE (1000 HZ PER CHANNEL) WITH A 100 MVPP TEST SIGNAL.

Freq. (Hz)	Meas. freq. (Hz)	dt ( $\mu$ s)	Crosstalk spec. (dB)	THD (%)	BCI online accuracy (%)
13	13.6	987 $\pm$ 37.7	-65.7	1.19	100
113	113.3	1001 $\pm$ 106	-68.0	0.41	100
223	222.7	1000 $\pm$ 3.85	-67.6	0.27	100

Freq. = Test frequency. Meas. freq. = Measured frequency as shown in PSD. dt = time between samples (ideal dt = 1000  $\mu$ s). Crosstalk spec. = PSD( $f, ch_1$ ) - PSD( $f, ch_i$ ) at the worst case. THD = total harmonic distortion.

standard. Training EEG was acquired by the system at 250 Hz/channel using the procedure described above. The subject was instructed to alternate between eyes open (state A) and eyes closed (state B).

Similar to the function generator test procedure, the online mode involved the subject alternating between 20-s periods of eyes open and 20-s periods of eyes closed conditions for a total of 200 s. The BCI system decoded the underlying EEG signals into either states and the performance was assessed as the percentage of correctly decoded samples.

## III. RESULTS

The BCI software occupied 101 kB (101 thousand bytes), and 180 kB was allocated to heap, where runtime variables were stored. The internal RAM capacity totaled 327 kB, which allows the remaining 46 kB to be used for future expansion of the BCI without the need for external RAM.

### A. Function Generator Test

The system was tested with sine waves at 13 Hz, 113 Hz, and 223 Hz to assess signal acquisition fidelity, and the results are summarized in Table I. Representative time and PSD plots are shown in Figs. 4 and 5, respectively. Since the crosstalk specification was below -65 dB for the 3 grounded channels, the mux encoding was deemed to be correct.

The ADC overhead was 59  $\mu$ s. The processing time overheads relative to each 2-s long data sample were as follows: 0.24% demux, 0.16% FFT, 14.5% PSD, and 1.23% binning. For instance, PSD calculations took 290 ms to process 2-s long data. The SD card writing significantly impacted the other DSP functions, since it caused 70–75 ms gaps in the recorded signals. Thus, this feature was disabled during the human EEG testing.

### B. Human EEG Test

After calibration, the state transition thresholds were found to be  $T_A=0.0125$  and  $T_B=0.99$ , which indicated a high level of separability between the EEG underlying the eyes open and closed states. Ideally  $T_A$  and  $T_B$  should be 0 and 1, respectively. During the online BCI test, the mean of  $P(B|f \in A)$  was  $0.00582 \pm 0.0297$ , while the mean of  $P(B|f \in B)$  was  $0.910 \pm 0.229$ . Note that the state machine eliminated false transitions from state B to A. This resulted in an overall online BCI decoding accuracy of 100%, indicating that over 200-s period, there were 100 correct decisions.

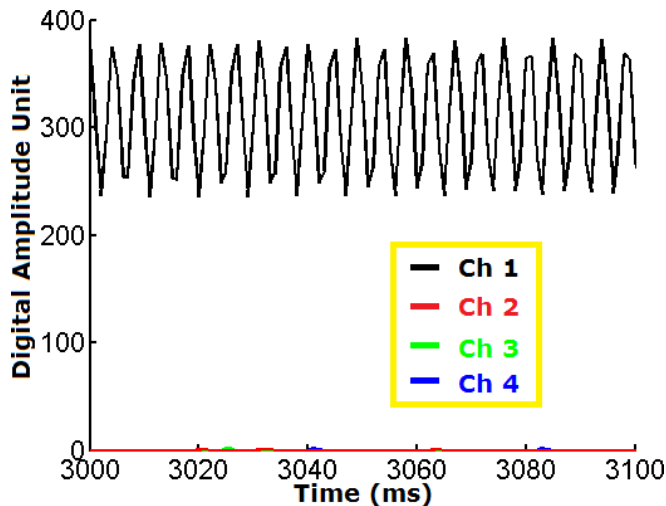


Fig. 4. Time domain plots. The sine wave (223 Hz) was only sent to Channel 1.

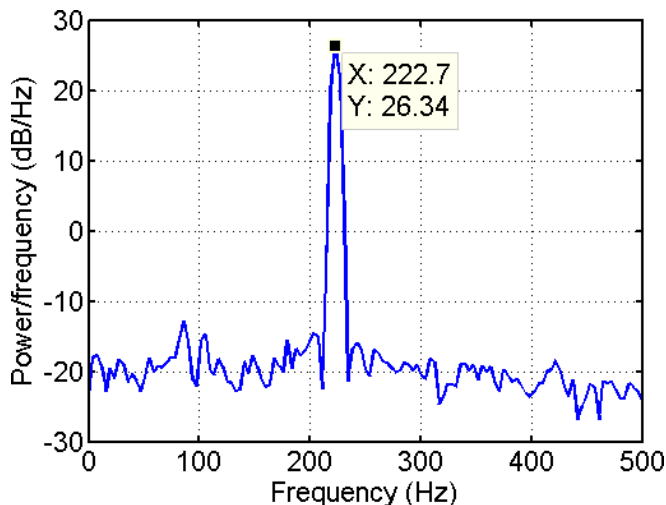


Fig. 5. Welch power spectrum for the sine wave test at 223 Hz on Channel 1. Note that the DC bias was removed first.

#### IV. DISCUSSION AND CONCLUSIONS

The current study demonstrates that it is possible to execute critical BCI functions, including EEG acquisition, processing, and decoding using a custom amplifier array, mux, and a commercial ULP DSP. Despite the limited computing resources available on the DSP, this BCI system is still capable of high fidelity recording and highly accurate decoding of brain signals. Furthermore, the capabilities and performances are similar to those running on full-sized computers with larger number of brain signal channels [10].

With the current configurations, the ULP DSP was estimated to consume up to 100 mW at full load and <10 mW during idle [11]. Based on preliminary simulations, the maximum power dissipation from a chest wall implant was within physiological tolerance. Also, a 1000-mAh battery can power the system for  $\sim 14$  h at full power or >100 h at idle power. Based on [12], a user is expected to operate the BCI at full power for 26.7% of a 24-h period, bringing the average

power consumption to 34 mW ( $\sim 38$  h on one charge).

Future work will involve integrating the DSP with our previously developed 64-channel amplifier array and mux [13] and a more efficient, custom-made ADC. The custom ADC should be able to circumvent the internal ADC overhead to allow high- $\gamma$  band acquisition on all 64 channels. Ultimately, this setup will be tested in a population of subjects with ECoG electrode implants. However, the utilization of 64 channels will most likely exceed the memory capacity of the DSP. Hence, more efficient implementations of the BCI algorithm, e.g. using streaming PCA [14], will be necessary. Also, various optimization procedures can further improve the efficiency of the BCI algorithm.

Finally, all of the necessary components will need to be implemented into a dedicated printed circuit board (PCB) for the CWU implant. Currently, it is estimated that these critical components will occupy  $\sim 5 \times 6$  cm<sup>2</sup>. This PCB area is similar to that of a commercial deep-brain stimulator CWU.

#### REFERENCES

- [1] Bickenbach J, editor. International Perspectives on Spinal Cord Injury. World Health Organization; 2013.
- [2] National Spinal Cord Injury Statistical Center (NSCIS). Spinal cord injury facts and figures at a glance - 2013;. National Spinal Cord Injury Statistical Center, Birmingham, Alabama.
- [3] Wang PT, King CE, McCrimmon CM, Lin JJ, Sazgar M, Hsu FPK, et al. Comparison of decoding resolution of standard and high-density electrocorticogram electrodes. *Journal of Neural Engineering*. 2016;13(2):026016.
- [4] Wang W, Collinger JL, Degenhart AD, Tyler-Kabara EC, Schwartz AB, Moran DW, et al. An electrocorticographic brain interface in an individual with tetraplegia. *PLoS One*. 2013;8(2):e55344.
- [5] Ando H, Takizawa K, Yoshida T, Matsushita K, Hirata M, Suzuki T. Wireless Multichannel Neural Recording With a 128-Mbps UWB Transmitter for an Implantable Brain-Machine Interfaces. *IEEE T Biomed Circ Sys*. 2015;.
- [6] Mestais CS, Charvet G, Sauter-Starace F, Foerster M, Ratel D, Benabid AL. WIMAGINE: Wireless 64-Channel ECoG Recording Implant for Long Term Clinical Applications. *IEEE T Biomed Circ Sys*. 2014;23(1):10–21.
- [7] Wang PT, King CE, Chui LA, Do AH, Nenadic Z. Self-paced braincomputer interface control of ambulation in a virtual reality environment. *J Neural Eng*. 2012;9(5):056016.
- [8] King CE, Wang PT, Chui LA, Do AH, Nenadic Z. Operation of a brain-computer interface walking simulator for individuals with spinal cord injury. *J Neuroeng Rehab*. 2013;10(1):1.
- [9] McCrimmon CM, Wang M, Lopes LS, Wang PT, Karimi-Bidhendi A, Liu CY, et al. A Small, Portable, Battery-Powered Brain-Computer Interface System for Motor Rehabilitation. In: 38th Annual International Conference of the IEEE Engineering in Medicine and Biology Society; 2016. In submission.
- [10] McCrimmon CM, King CE, Wang PT, Cramer SC, Nenadic Z, Do AH. Brain-controlled functional electrical stimulation therapy for gait rehabilitation after stroke: a safety study. *J Neuroeng Rehab*. 2015;12(1):57.
- [11] TMS320C5517 Power Consumption Summary; 2015. Available from: [http://processors.wiki.ti.com/index.php/TMS320C5517\\_Power\\_Consumption\\_Summary](http://processors.wiki.ti.com/index.php/TMS320C5517_Power_Consumption_Summary).
- [12] Matthews CE, Chen KY, Freedson PS, Buchowski MS, Beech BM, Pate RR, et al. Amount of time spent in sedentary behaviors in the United States, 2003–2004. *Am J Epidemiol*. 2007;167(7):875–881.
- [13] Mahajan A, Karimi-Bidhendi A, Wang PT, McCrimmon CM, Liu CY, Nenadic Z, et al. A 64-channel ultra-low power bioelectric signal acquisition system for brain-computer interface. In: *IEEE Biomedical Circuits and Systems Conference (BioCAS) 2015*; 2015. .
- [14] Mitliagkas I, Caramanis C, Jain P. Memory Limited, Streaming PCA. *arXiv*. 2013;1307.0032v1.